AN ACCURATE AND COMPUTATIONALLY EFFICIENT SMALL-SCALE NONLINEAR FEA OF FLEXIBLE RISERS

M.T. RAHMATI, H.BAHAI, G. ALFANO

Department of Mechanical, Aerospace and Civil Engineering

Brunel University, Uxbridge, UB8 3PH, UK

mt.rahmati@brunel.ac.uk

Keywords: Flexible risers, frictional contact, periodic boundary condition, FE modelling

ABSTRACT

This paper presents a highly efficient small-scale, detailed finite-element modelling method for flexible risers which can be effectively implemented in a fully-nested (FE^2) multiscale analysis based on computational homogenization. By exploiting cyclic symmetry and applying periodic boundary conditions, only a small fraction of a flexible pipe is used for a detailed nonlinear finite-element analysis at the small scale. In this model, using three-dimensional elements, all layer components are individually modelled and a surface-to-surface frictional contact model is used to simulate their interaction. The approach is applied on a 5-layered pipe made of inner, outer and intermediate polymer layers and two intermediate armour layers, each made of 40 steel tendons. The capability of the method in capturing the detailed nonlinear effects and the great advantage in terms of significant CPU time saving are demonstrated by comparing the results obtained on elements of pipe of different lengths, equal to one pitch length L_p as well as $L_p/5$, $L_p/20$ and $L_p/40$.

1. INTRODUCTION

Unbonded flexible risers have become the main means for transporting oil and gas between the seabed and surface in ultra-deep waters. They consist of several polymer and steel layers that can move internally relative to each other. This gives them low bending stiffness and makes them highly valuable tools for subsea oil and gas companies. Their ability of withstanding large displacements and rotations makes them ideal for floating platforms. Due to the complex internal dynamics of flexible risers related to the possible interlayer slip, however, the conventional stress prediction and fatigue analysis tools based on simplified analytical formulations and linear methods have a limited

degree of accuracy. In many problems of very significant industrial interest, including but not limited to fatigue-life prediction and life extension for existing risers or forensic analyses after major accidents, sufficient accuracy can only be obtained by the use of models that properly take into account contact and friction between layers and how these are related to internal and external pressure, bending and torsion of individual tendons, large displacements and rotations [1].

Major established industries in the field rely on computational mechanics software to analyze and design flexible pipes. In few cases the finite difference method (FDM) is used to discretize the model in space [2]. Here, the focus will be on the finite element method (FEM), which is the most widely used approach as it is capable of handling geometrically complicated domains, a variety of boundary conditions, nonlinearities, and coupled phenomena that are common in flexible risers.

A number of authors have developed various finite-element (FE) modelling approaches for flexible pipes. de Sousa et al. [3] and Merino et al. [4] describe a model using a commercial FE package with concentric solid layers discretised with thin-walled 4-noded shells. The carcass and pressure armour layers are modelled as equivalent cylindrical layers with orthotropic properties, for which analytical derivations are presented. Tendons are modelled as three-dimensional Euler-Bernoulli beams, with principal axes (for moment calculations) in the pipe radial direction, and a penalty method for contact constraint enforcement is used. A similar approach using a general purpose FE program is adopted by Le Corre and Probyn [5]. In this model of a single-core umbilical, three concentric sheaths are modelled as cylindrical shells. The annulus between each pair of sheaths contains helically wound tubes and cables modelled as circular-section beams. Simulations are carried out using an explicit-dynamics solution procedure, with a general contact algorithm to include all parts with a friction coefficient derived from tests. Although FE models can account for the complex internal structure of flexible risers, their computational requirements limit their applicability to just a few meters in length at most. So, a more efficient methodology with lower computational cost is required to bridge the gap between nonlinear dynamic simulations at the large scale and detailed finite element models at the small scale.

One approach to reduce computational cost of the analysis of flexible risers is to develop constitutive laws for large-scale beam models, which link generalised stresses and strains to model the hysteresis loops occurring for flexible pipes subjected to cyclic loading, as shown by Tan et al. [6]. Using these constitutive laws a nonlinear bending stiffness of the pipe, which captures the transition from no-slipping to slipping between layers, can be included in the analysis. Due to the close analogy between the aforementioned hysteretic response and the elasto-plastic behaviour of metal beams, this hysteretic response can be modelled as a rate-independent elasto-plastic relationship between generalised strains and stresses. Following this approach, Sævik [7, 8] presents a FE model for predicting stresses due to axisymmetric loads and bending loads in flexible pipes.

The interlayer stick-slip behaviour due to friction is taken into account by formulating a constitutive relation based on a plastic beam model, with nonlinear stiffness derived from an analytical formulation in terms of the moment resultants and the wire slips. Experimental studies on the model using strain measurements showed that the numerical distribution of the longitudinal stress predicted by the method is in reasonable agreement with the measured data. A similar approach is used by Alfano et al. [9], building on the analogy between frictional slipping between different layers of a flexible riser and frictional slipping between micro-planes of a continuum medium in non-associative elasto-plasticity. In this way, a linear elastic relationship was used for the initial response, in which no slip occurs, and a non-associative rule with linear kinematic hardening was then introduced to model the full-slip phase. Using this approach, the above authors conducted several analyses using a detailed FE model at the small scale to estimate the input parameters of the beam-constitutive model at the large scale.

Key to accurate solution of the small scale FE problem is the use of suitable boundary conditions. Various boundary conditions can be used, including zero fluctuations over the whole model, uniform displacement, uniform traction and periodic boundary conditions [10]. The periodic boundary conditions are the most effective and accurate for most cases involving a periodic microstructure or when the microstructure is not periodic but the small scale model is sufficiently statistically representative [11, 12]. Leroy et al. [13], in their FE model of a flexible pipe, assume periodic solutions (given constant curvature in the pipe) and determine an analytical solution of equilibrium of wires on a torus (the bent pipe). The 3D periodic model consisted of a single layer of helical wires, with all internal and external layers represented by rigid kernels. They also developed a detailed FE model of a full pitch length of the pipe, solved using explicit dynamics. Cross-validation between the models was carried out for cyclic bending and a comparison of the axial stress distributions showed good correlation for the inner armour layer.

In their analysis of one-pitch long segment of a flexible riser using a detailed FE model, which includes all layers in frictional contact between each other, Edmans et al. [14, 15] studied the influence of boundary conditions by considering two cases. In one case fixed in-plane boundary conditions are used, whereby the displacements of the nodes of two end-cross sections are prescribed so that the two cross sections undergo a rigid relative displacement and rotation. In a second case, periodic boundary conditions are used, whereby, in addition to the relative displacement and rotation between the two end cross sections, additional displacement (fluctuations) are allowed for all nodes of the cross section, with the constraint that the fluctuations must be the same for two nodes of either end cross section with the same position in the cross section. The comparison between the two types of boundary conditions, in a case in which the one-pitch long riser segment is subject to prescribed bending, shows that fixed in-plane boundary

conditions result in a much stiffer response [14] and significant spurious edge effects, with stress concentrations building close to the two end sections [15], whereas periodic boundary conditions lead to a much more realistic stress distribution that is uniform across the longitudinal direction.

One major challenge in using the constitutive law based on the non-associative elasto-plasticity analogy is the determination of the parameters of the constitutive law to bridge the small scale of the detailed FE simulations with the large scale of the model accurately. An alternative approach which does not have this limitation is a fully-nested multi-scale procedure [16], currently in widespread use for the modelling of composite materials. With this method, at each integration point (i.e. cross section) of the large-scale beam model, the stress resultants corresponding to assigned generalised strains are determined through the solution of the small-scale FE problem. This requires recasting the computational homogenisation problem in a more general theory which can link different structural models at different scales [17, 18].

When FE models are used at both scales, the fully nested procedure is also known as the FE^2 method. This name very clearly highlights the significant computational cost associated with fully nested computational homogenisation, because, in an implicit incremental solution strategy, the nonlinear small-scale FE model is to be solved at each integration point of the large-scale model, at each equilibrium iteration conducted within each increment of the analysis. For this reason, a fully nested approach is often used only for 'hot-spots', i.e. critical areas of the structure where significant accuracy is needed [16].

On the other hand, even a long riser can be modelled at the large scale with reasonably good accuracy using hundreds or few thousands nodes and integration points. Therefore, the solution of the linear system at each equilibrium equation is normally not an issue. The assembly of the residual vector and tangent stiffness matrix is where the small-scale detailed FE models have to be solved at each integration point, but this is the 'perfectly scalable' part of the process if parallel computing is used, because there is no need for any exchange of information between small-scale analyses at different integration points. Therefore, a fully nested procedure can be feasible if the computational cost of the small-scale model is made sufficiently small so that it can be effectively run within one single node of a cluster in a limited amount of time.

Hence, building on some preliminary work done for an extremely simplified riser made of only two polymer layers and one armour layer [19], this paper describes an efficient modelling approach for the small-scale analysis of a more realistic flexible riser made of 3 polymer layers and 2 armour layers. It also explains how cyclic symmetry of the riser can be exploited by writing periodic boundary conditions based on the multiscale theory derived by Edmans et al. [18] for the case when different structural models are used at different scales. This results in periodic boundary conditions,

written in terms of dummy nodes, which are different from those used in the aforementioned work by Leroy et al. [13].

We consider a riser for which the pitch length of the tendons is the same in both the inner and the outer armour layers, which is a condition very close to the real design of risers. This means that, apart from the carcass and the pressure armour layer, if the latter is present, denoting by L_p the pitch length of each tendon and by N the number of tendons, the geometries of two cross sections at a distance L_p/N, or multiple of it, is the same. The carcass and the pressure armour layer are typically made of a single tendon wound at a small pitch with an interlocking mechanism that prevents unwinding. In general, these layers do not present the same cyclic symmetry. However, while their radial stiffness is significant, their extensional and bending stiffness can be normally considered negligible. Furthermore, it is widely accepted that they can be effectively modelled as a continuum pipe made of orthotropic material, with the longitudinal axis as one of the material directions. Therefore, with this assumption, by definition they do not violate the cyclic symmetry of the riser.

On the other hand, one problem that has not been considered in previous work is that uniqueness of the solution cannot guaranteed in the presence of friction [20]. The probability of bifurcations is expected to increase with the number of layers because of the increase in the surfaces where frictional slips occur. To address this issue, various riser models with different lengths starting from the smallest repeat of unit of length equal to L_p/N to a model pitch length L_p are used. The results have been compared and discussed.

The structure of the paper is as follows. Section 2 describes how the fully-nested (FE^2) computational homogenization method can be applied to flexible risers using the extended theory presented by Edmans et al. [18]. The FE models for the small-scale analysis of risers of different lengths are described in Section 3; in particular, the implementation of periodic boundary conditions is discussed in detail in Section 3.1. In Section 4, the differences in numerical results and CPU time obtained by using models of different lengths are reported and discussed to evaluate the accuracy and the computational saving entailed by the use of the smaller and smaller 'slices' of repeating units of riser. The effectiveness of the use of periodic boundary conditions is also assessed further, by comparing results obtained with periodic and fixed in-plane boundary conditions. Finally, conclusive remarks are made and future work discussed in Section 5.

2. FULLY NESTED MULTISCALE ANALYSIS OF RISERS

A fully-nested computational homogenization scheme is essentially based on the construction of a micro-scale (or more generally small-scale) boundary-value problem (BVP) at each integration

point of a macro (or large-scale) model. In particular, this 'micro' problem is defined for a suitably defined representative volume element (RVE) of the micro scale and is solved numerically to determine the constitutive response of the material at each integration point.

For the flexible risers considered in this paper, a 3D continuum model is used at the small scale, which is to be linked to a large-scale beam model, where generalised strains and stress resultants are employed. This means that different structural models are used at different scales, which makes classical computational homogenisation, e.g. [16], not directly applicable as shown in detail by Edmans et al. [18], where an extension of that theory has been formulated. Referring to the original paper for the details of the derivation, a geometrically non-linear formulation is assumed at the large scale: in particular, it is assumed that displacements and rotations are large, while macro strains are small enough so that a geometrically linear formulation can be adopted at the small scale. The small-scale problem is then written in its general form as follows:

$$\begin{cases} Q_{bc}u_m = Q_{bc}\overline{P}\,\varepsilon_M \\ \langle\, \sigma_m(B_m u_m), B_m \delta u_m \,\rangle = 0 \qquad \forall \delta u_m : Q_{bc}\delta u_m = 0 \end{cases} \tag{1}$$

In this equation, $\overline{P}$ is a linear operator that translates the large-scale strain ε_M at the integration point into a corresponding small-scale displacement field v_m, Q_{bc} is a suitably defined operator that extracts the appropriate boundary values of a small-scale displacement field, so that Equation $(1)_1$ represents the boundary conditions on the RVE; B_m is the linear operator mapping the micro strains to the micro displacement field; σ_m is the micro stress field and $\sigma_m(\varepsilon_m)$ denotes the constitutive equation at the small scale, that in the case of a flexible riser is in general nonlinear because of the unilateral frictional contact between the different components of the flexible riser; finally, symbol $\langle\, x, y \rangle$ in Equation $(1)_2$ represents the virtual work computed by a stress field x for a virtual strain field y. Therefore, Equation $(1)_2$ is the variational enforcement of equilibrium in the RVE, which is done approximately here because a FE model is used at the small scale.

Given a large-scale strain ε_M, the small-scale problem consists of finding a small-scale displacement field u_m solution of the variational problem (1). In practice, for each RVE a dummy reference node R is introduced, whose degrees of freedom are collected in a vector $\eta_{MR} = \varepsilon_M$, which therefore represents the components of the macro strain. Therefore Equation (1) becomes:

$$\begin{cases} Q_{bc}u_m = Q_{bc}\overline{P}\,\eta_{MR} \\ \langle\, \sigma_m(B_m u_m), B_m \delta u_m \,\rangle = 0 \qquad \forall \delta u_m : Q_{bc}\delta u_m = 0 \end{cases} \tag{2}$$

Once the micro-stresses σ_m are computed in (2), by using a 'generalised Hill condition' (GHC) enforcing the equality of the virtual works at the two scales [18], the macro-stress σ_M is computed via the following variational equation:

$$\langle \sigma_M, \delta\eta_{MR} \rangle = \langle \sigma_m, B_m \delta u_m \rangle \qquad \forall\, \delta\eta_{MR} \epsilon\, D_M \quad \forall\, \delta u_m : Q_{bc} \delta u_m = Q_{bc} \overline{P}\, \delta\eta_{MR} \tag{3}$$

which, in practice, means that σ_M is simply obtained as the nodal reaction vector at the dummy reference node.

The practical implementation of Equation (2) in the small-scale FE model of a segment of riser is described in the next section.

3. SMALL-SCALE FINITE-ELEMENT MODELS OF SEGMENTS OF RISER

A simplified 5-layer flexible pipe, made of three polymer layers and two armour layers, was considered. Both the inner and the outer armour layers are made of 40 steel tendons, with rectangular cross section, which are wound with the same pitch length L_p equal to 320mm. The model is created using the FE package ABAQUS, version 6.13.1. All components are modelled with fully-integrated 8-noded 3D solid elements with incompatible strains [21], with surface-to-surface frictional contact between all components.

As previously discussed, it is widely accepted that the use of periodic boundary conditions in multiscale computational homogenization provides the most accurate results, at least at sufficient distance from the real boundary of the structure. On the other hand, the solution for a segment of riser whose length is any multiple of L_p/N should be characterized by the same cyclic symmetry if periodic boundary conditions are applied and if such solution is unique. Therefore a small 'slice' of riser with the minimum length L_p/N could be used in the analysis, instead of using, for example one entire pitch length L_p, as was done in [14, 15].

However, uniqueness of the solution in problems involving frictional contact is still an open issue [20]. Bifurcations can potentially occur and some mathematical studies have related the possible non-uniqueness of the solution to the size of the mesh and to the values of the friction coefficient [20, 22]. While a rigorous mathematical analysis aiming to investigate the existence of bifurcations and, if they do exist, their nature, is outside the scope of this paper, potential non-uniqueness can result in different solutions when segments of pipes whose lengths are different multiples of L_p/N are considered. This issue is addressed here by conducting different analyses with segments of risers of length equal to L_p/N, with $N = 1, 5, 20, 40$, as shown in Figure 1 and comparing the results. By considering different lengths, it is also possible to quantify the decrease in CPU time associated with the reduction of the length of riser analyzed.

For each model, Table 1 reports the length and the number of nodes. In Table 2, for each layer of the smallest model, the number of elements in the axial and circumferential directions and the total number of elements are given. For each layer, the inner and outer radii, r_0 and r_1, the material, the Young's modulus and Poisson's ratio, are reported in Table 2. The cross section of the model is

shown in Figure 2(a) and tendon layers arrangements for the smallest model are shown in Figure 2(b).

Table 1: Length, number of nodes and elements of the models.

Model	Model length L (mm)	No. of Nodes	No. of Elements
a	8	12660	4744
b	16	24521	9168
c	64	87209	36672
d	320	419334	183200

The smallest model has a length equal to $1/40$ of the pitch length of the tendons. For this small slice of pipe the position of each tendon on one end cross section is the same as the position of the adjacent tendon on the other end cross section. As discussed in the previous section, this makes this slice of $1/40$ of length the smallest repeating unit of the pipe. Furthermore, as typical in first-order computational homogenisation, the assumption is made that the variations of the internal stress resultant (i.e. large-scale stress) and of the generalised strain (i.e. large-scale strain) are small enough that, for the element of pipe under consideration, they can be neglected. Therefore, to within a rigid motion, the assumption of periodic kinematics is made, resulting in the enforcement of periodic boundary conditions.

Table 2: Number of elements in each layer (circumferentially and axially)

Layer	Type	Axial/helical direction	Circumferential direction	Total No. of elements
1	Polymer	4	156	624
2	Armour	8	160	1280
3	Polymer	4	169	676
4	Armour	9	160	1440
5	Polymer	4	181	724

The study in this paper focuses on cases in which the segments of pipes are subject to bending, as well as internal and external pressure, the latter being balanced to produce a relatively small and outward radial displacement of the inner surface of the inner polymer layer (inner liner). While a carcass layer is present in most designs of flexible risers, it is typically not a leak proof layer, whereby the internal pressure is applied to the inner liner. As a result, the carcass would remain undeformed under the load cases considered in our analysis and for this reason it has been not

considered in the models. Furthermore, we did not consider the presence of a pressure armour layer because this is not present in all risers and we wanted to limit the complexity of the analysis, by focusing on proof-of-concept, yet realistic case studies.

A fully-implicit nonlinear static analysis based on the Newton-Raphson method is used to solve the models. The analyses were carried out in parallel on a computer cluster with two dual-core 1.8 GHz processors (32 processors in total) using 8MB of RAM. Whilst the run time for the smallest model is only few minutes, it takes over 26 hours to complete the analysis of a model with one pitch length.

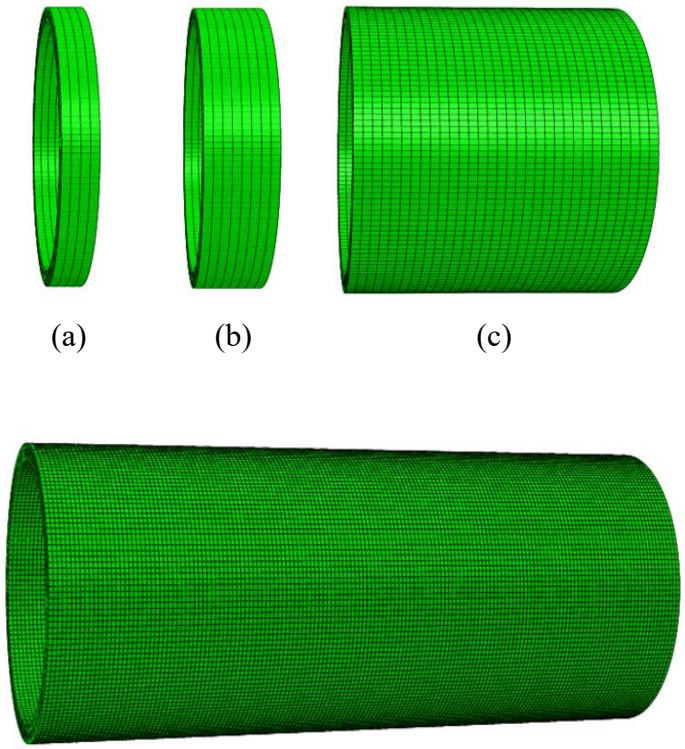

Figure 1: FE models with lengths equal to (a) $L_p/40$, (b) $L_p/20$, (c) $L_p/5$ and (d) L_p, L_p being the pitch length of the steel tendons.

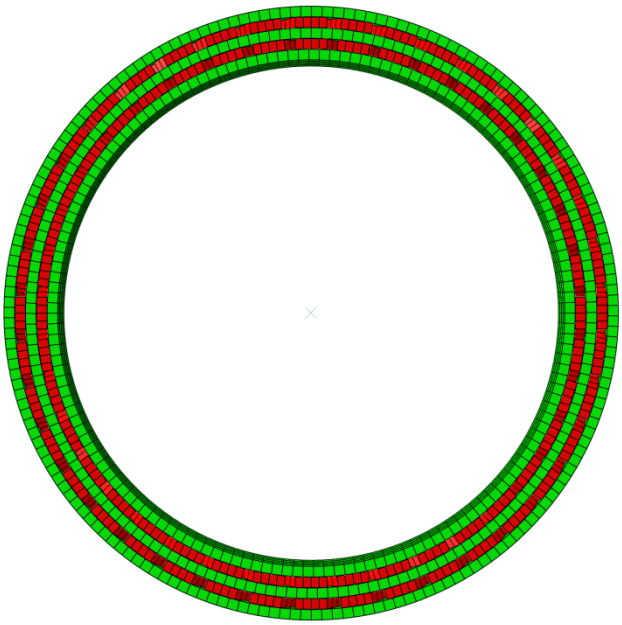

(a) Cross section of the model.

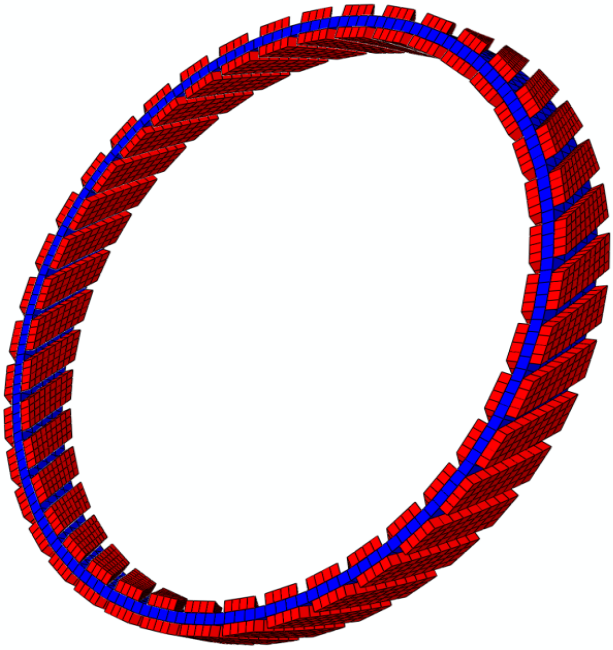

(b) Tendon layers arrangement in the model.

Figure 2: The smallest FE model.

Table 3: Dimensions and material properties of components in the model.

Layer	r_0, r_1 (mm)	Material	E (MPa)	υ
1	48, 50	Polyethylene	0.35	0.4
2	50, 52	Carbon Steel	210	0.3
3	52, 54	Polyethylene	0.35	0.4
4	54, 56	Carbon Steel	210	0.3
5	56, 58	Polyethylene	0.35	0.4

The contact model used is a surface-to-surface finite-sliding formulation where separation and sliding of finite amplitude and arbitrary rotation of the surfaces may arise. Based on the data associated with the specified contact pairs, a contact element is generated. At each integration point these elements determine a measure of over-closure (penetration of the point on the surface of the deforming body into the rigid surface) and of relative shear sliding. These kinematic measures are then used, together with appropriate Lagrange multiplier techniques, to introduce surface contact and friction.

The contact pressure, p, between two surfaces at a point is the sum of two components, p_c and p_d [22]:

$$p = p_c + p_d \tag{4}$$

where p_c is a function of the 'over closure', h, of the surfaces (the interpenetration of the surfaces) and p_d is regularization term.

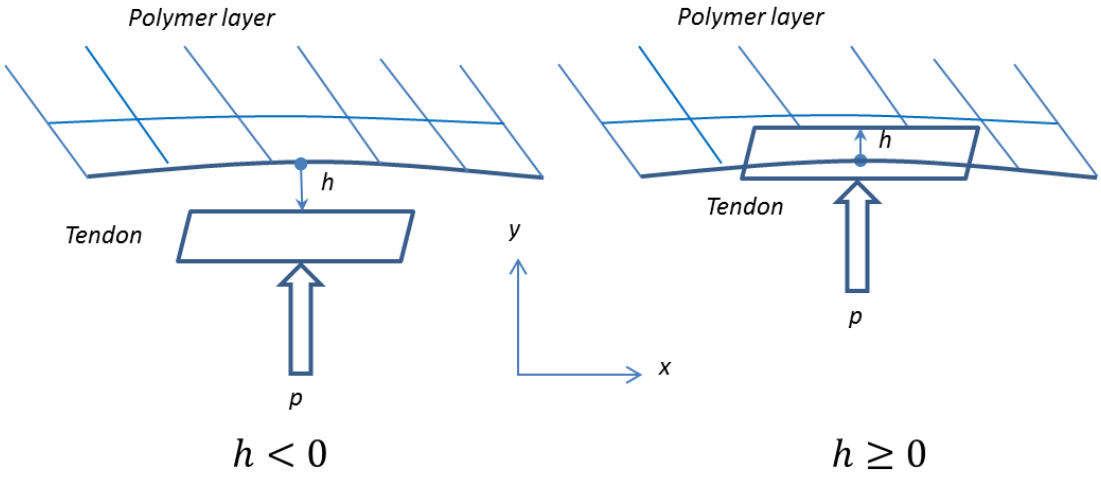

Figure 3: Contact modelling.

A 'hard' contact model in the normal direction was used whereby, if $h < 0$, there is no contact between the surfaces $p_c = 0$. If $h \geq 0$, the surfaces are in contact, see Figure 3 and p_c is then calculated as a Lagrange multiplier, using a penalty method [22]. A Coulomb friction model is used, assuming for the friction coefficient a value of 0.16.

The regularization term, p_d, is used to avoid convergence difficulties arising due to the sudden violation of contact constraints. It is obtained as a 'viscous' pressure that is a function of the normal relative velocity, $\dot{h}$, at which the surfaces approach or separate from each other, and of a damping coefficient γ, which in turn is a function of h:

$$p_d = p_d(h, \dot{h}) = \gamma(h)\dot{h} \tag{5}$$

The damping coefficient, γ, was generated automatically by the program and then scaled down by a factor ranging between 1 and 10. It was checked that varying this scaling factor does not influence the results.

4 IMPLEMENTATION OF PERIODIC BOUNDARY CONDITIONS

Due to cyclic symmetry and since the length of each model is a multiple of L_p/N, for each one of the considered models there is a one-to-one correspondence between the nodes of the two end cross sections that have the same position in the plane of the un-deformed cross-section. Therefore, denoting by N_c the number of nodes on either end cross section, N_c pairs of nodes are defined by this correspondence. Following [17, 18], for each one of these pairs of nodes, a new 'dummy' projected node is introduced on a plane which is parallel to the end cross section in their un-deformed configuration. This is shown in Figure 4, where, for the generic pair of nodes, n_L and n_R indicate the corresponding nodes on the left-hand and right-hand end cross section, respectively, and n_P denotes the corresponding projected node.

A set of linear constraint equations was then generated, relating the degrees of freedom of each pair of nodes on the two end cross section to those of the corresponding projected node. The link is enforced for all displacement components U_n^i and rotation components ϕ_n^i of a node n, as follows:

$$U_{n_L}^i - U_{n_R}^i = U_{n_P}^i \qquad i = 1,2,3 \tag{6}$$

$$\phi_{n_L}^i - \phi_{n_R}^i = \phi_{n_P}^i \qquad i = 1,2,3 \tag{7}$$

It is worth noting that, in ABAQUS, a linear constraint equations between three degrees of freedom, d_1, d_2 and d_3, are written in the form:

$$\alpha_1 d_1 + \alpha_2 d_2 + \alpha_3 d_3 = 0 \tag{8}$$

where α_1, α_2 and α_3 are real coefficients. Therefore, for example, Equations (6) are implemented by choosing $d_1 = U_{n_L}^i$, $d_2 = U_{n_R}^i$ and $d_3 = U_{n_P}^i$, and by setting $\alpha_1 = 1$, $\alpha_2 = -1$ and $\alpha_3 = -1$, for $i = 1,2,3$. An analogous procedure is used for Equations (7).

The displacement and rotation vectors, $\boldsymbol{U}_{n_P}$ and $\boldsymbol{\phi}_{n_P}$ of each dummy projected node n_P are rigidly constrained to the displacement and rotation vectors, $\boldsymbol{U}_{R_P}$ and $\boldsymbol{\phi}_{R_P}$, of a projected reference point R_P at their center, using the following rigid-body constraint equations:

$$\boldsymbol{U}_{n_P} = \boldsymbol{U}_{R_P} + \boldsymbol{\phi}_{R_P} \times \boldsymbol{X}_{n_P} \tag{9}$$

$$\boldsymbol{\phi}_{n_P} = \boldsymbol{\phi}_{R_P} \tag{10}$$

where $\boldsymbol{X}_{n_P}$ indicates the position vector of the projected node n_P with respect to the reference point and $\times$ denotes the standard cross product of two vectors.

In this way, displacements and rotations of the reference point correspond to generalised strain components in the model [17, 18]. For example, prescribing a rotation ϕ_{R_P} of the reference point about one axis in the cross section is equivalent to prescribing periodic boundary conditions corresponding to a bending curvature equal to ϕ_{R_P}/L, L being the length of the model.

In other words, the vector η_{MR} appearing in Equation (2) and, in its variation, in Equation (3), is here given by:

$$\eta_{MR} = \begin{bmatrix} \boldsymbol{U}_{R_P} \\ \boldsymbol{\phi}_{R_P} \end{bmatrix} = \begin{bmatrix} U_{R_P x} \\ U_{R_P y} \\ U_{R_P z} \\ \phi_{R_P x} \\ \phi_{R_P x} \\ \phi_{R_P x} \end{bmatrix} \tag{11}$$

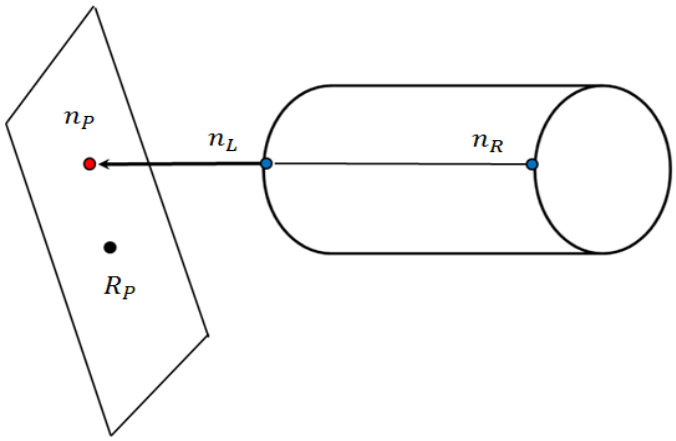

Figure 4: Correspondence between a pair of nodes n_L and n_R on the two end-cross sections and the dummy projected node n_P, which is constrained to the reference node R_P.

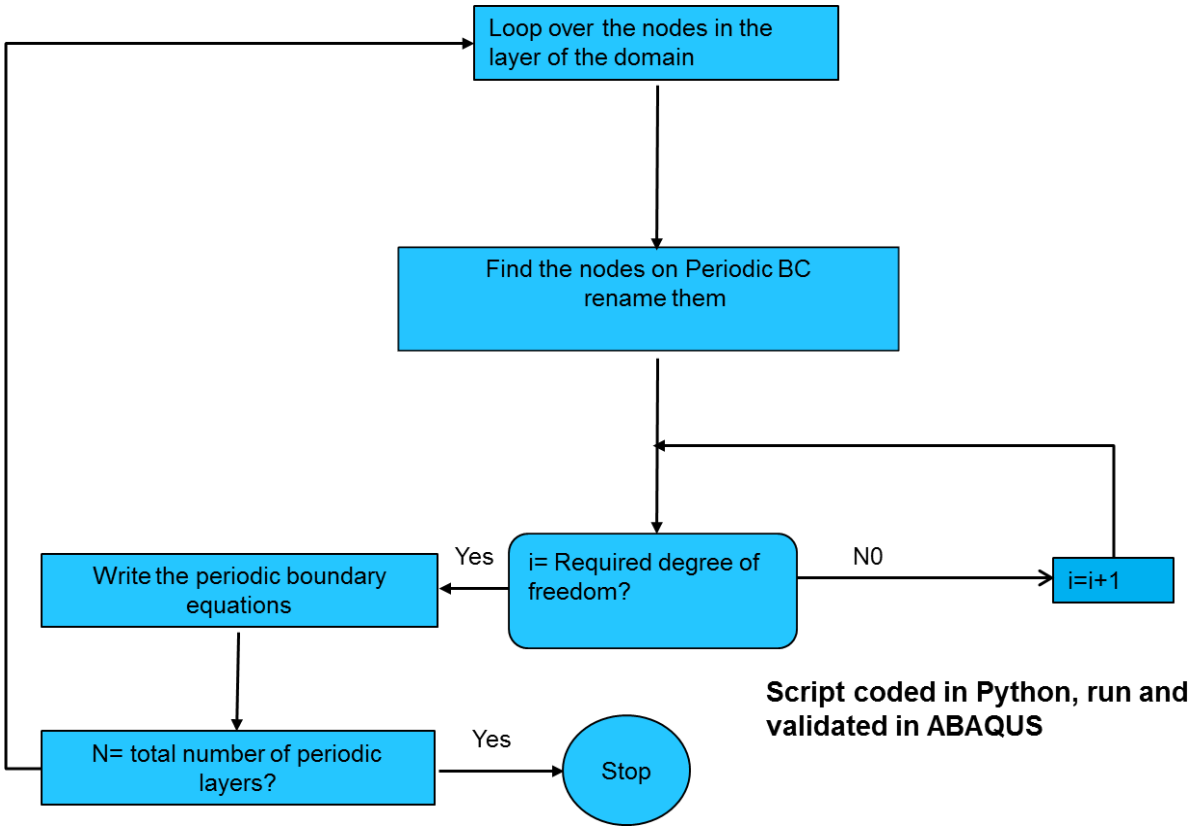

Figure 5: Flowchart of the implementation of periodic boundary conditions.

The flowchart describing the implementation of periodic boundary conditions is shown in Figure 5.

5. NUMERICAL RESULTS

The analyses were conducted by applying internal and external pressure in a first step, after which one symmetric cyclic history of bending curvature was prescribed, the maximum and minimum curvatures being 0.125 and -0.125 m^{-1}. In a first case the internal and external pressure were equal to 2 and 2.25 MPa, respectively. In a second case both values were doubled to 4 and 4.5 MPa, respectively. The curves in Figures 6 and 7 show the bending moment against the (prescribed) bending curvature for all models. It can be appreciated that the difference in the results of the models with different lengths is very small for both considered cases. The very small deviations can be attributed to bifurcations in the equilibrium paths, which in reality would not be found because of the inevitable imperfections within a real riser. These results confirm that use of the smallest repeating unit at the small scale of a multi-scale analysis is a valid choice.

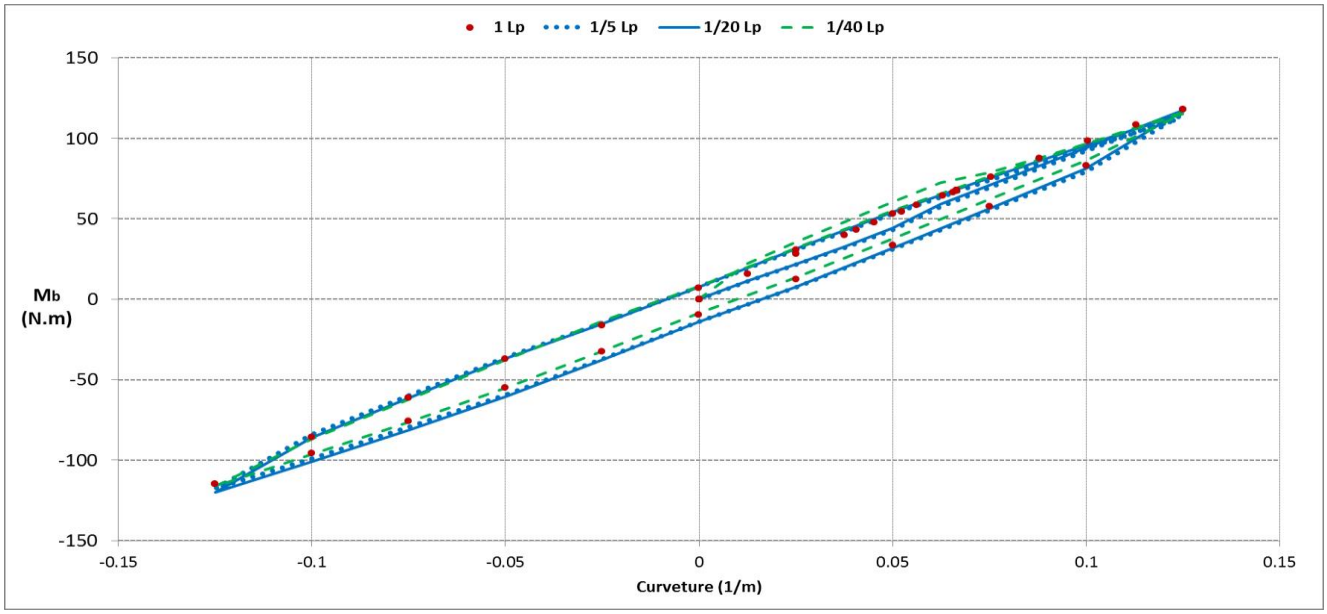

Figure 6: Bending moment vs prescribed bending curvature (internal pressure 2MPa, external pressure 2.25MPa).

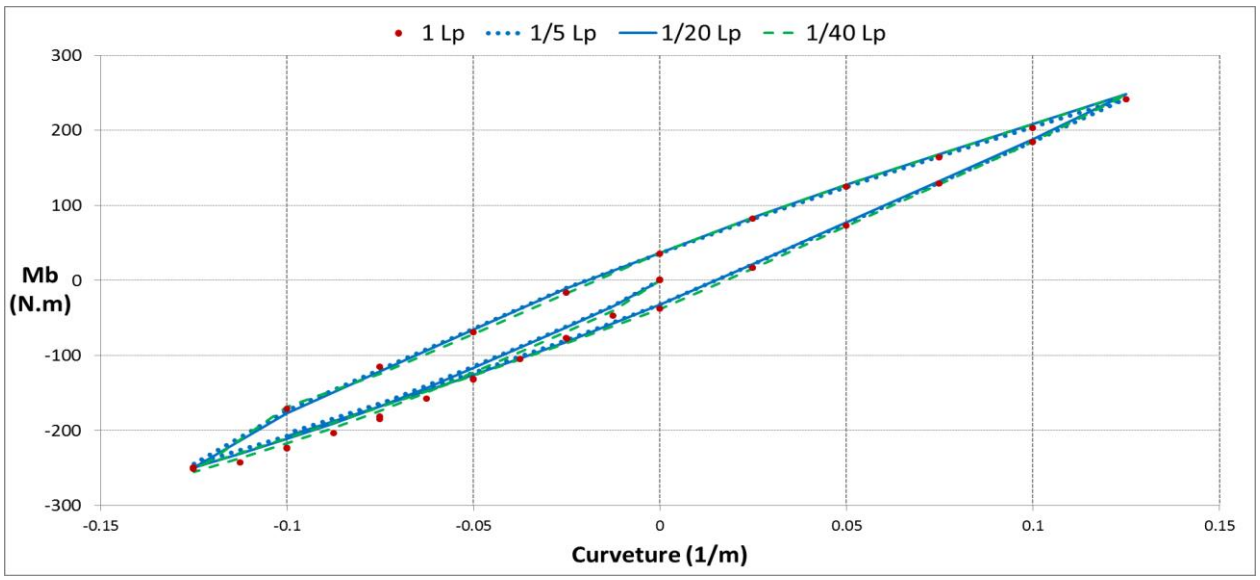

Figure 7: Bending moment vs prescribed bending curvature (internal pressure 4MPa, external pressure 4.5MPa).

Figure 8 shows that higher values of the pressure result in a stiffer response and a more marked hysteresis, as expected.

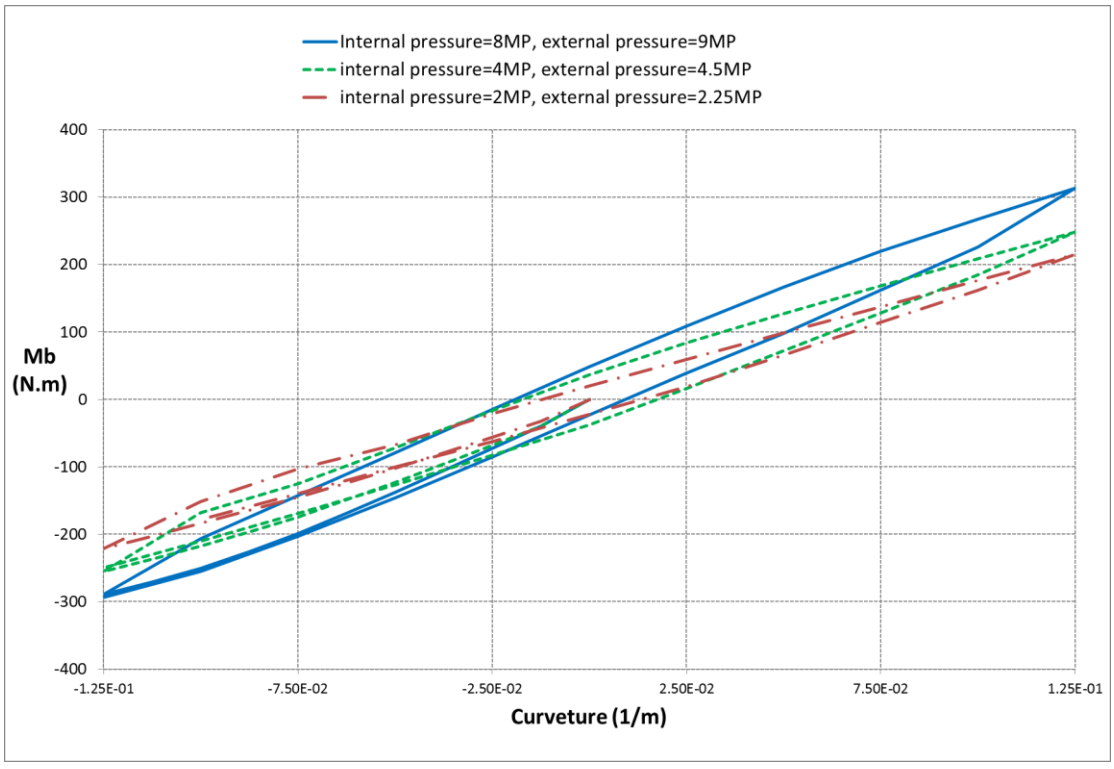

Figure 8: Bending moment vs prescribed curvature for the smallest length and three different values of the internal and external pressures.

The key role played by the periodic boundary conditions is shown in the results reported in Figures 9-11, which show the contour plots of the stress for the armour layer and for the outer and

inner layers, respectively. With fixed in-plane boundary conditions, tendons cannot slip or rotate with respect to the polymer layers at the two ends of the model. This produces reactive bending moments on the tendons resulting in spurious stress concentrations close to the end sections, which make the stress profile vary between the end sections and the mid-section of the riser segment, as can be appreciate in Figures 9(a), 10(a) and 11(a). Instead, with periodic boundary conditions, the stress profiles in Figures 9(b), 10(b) and 11(b) is practically the same at each cross section.

Figures 12 show the difference in the bending moment vs bending curvatures for the longest model. In Figure 13, it can be seen that fixed in-plane boundary conditions result in a much stiffer response and significant spurious edge effects, with stress concentrations building close to the two end sections. The reason is that, since the tendons cannot slip or rotate with respect to the polymer layers at the two ends of the model, they do not have enough length between the two fixed ends to deform in the way they do in reality. Since edge effects are felt in a volume whose size is independent on the model length, the shorter the model the higher is the stiffness when fixed in-plane boundary conditions are used. Instead, the models with periodic boundary condition capture the hysteretic response even with the smallest unit.

Figure 14 highlights the huge saving in CPU time, from 1600 minutes for the longest model of one pitch length (considered in the past in [14, 15]) to only few minutes for the smallest model. This confirms that the latter should be used in a nested multi-scale strategy.

(a)

(b)

Figure 9: Von Mises stress on helical armour wires using (a) fixed in-plane boundary conditions and (b) periodic boundary conditions.

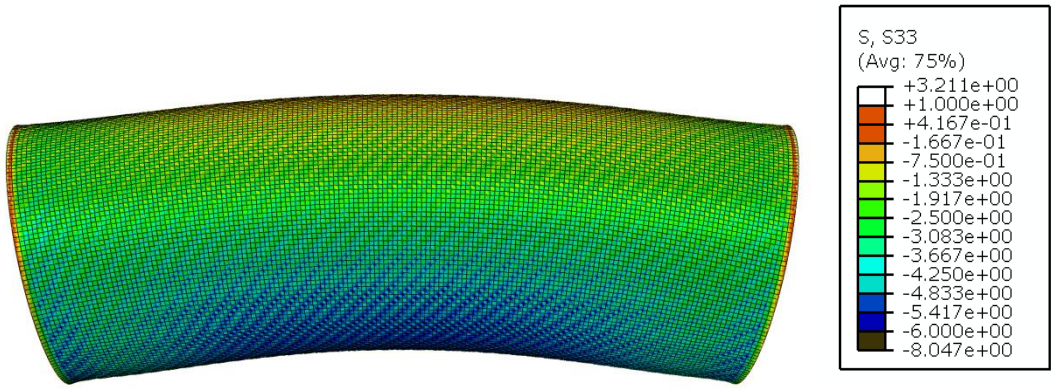

(a)

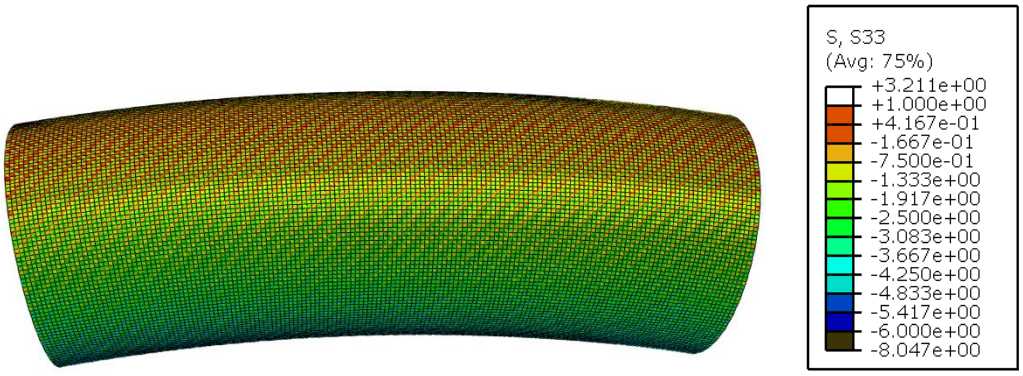

(b)

Figure 10: Axial stress on the outer layer using (a) fixed in-plane boundary conditions and (b) periodic boundary conditions.

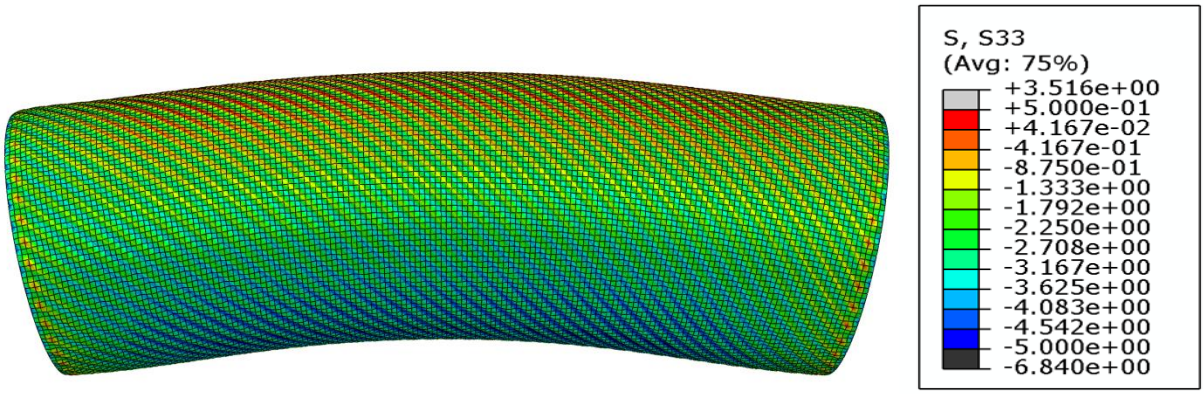

(a)

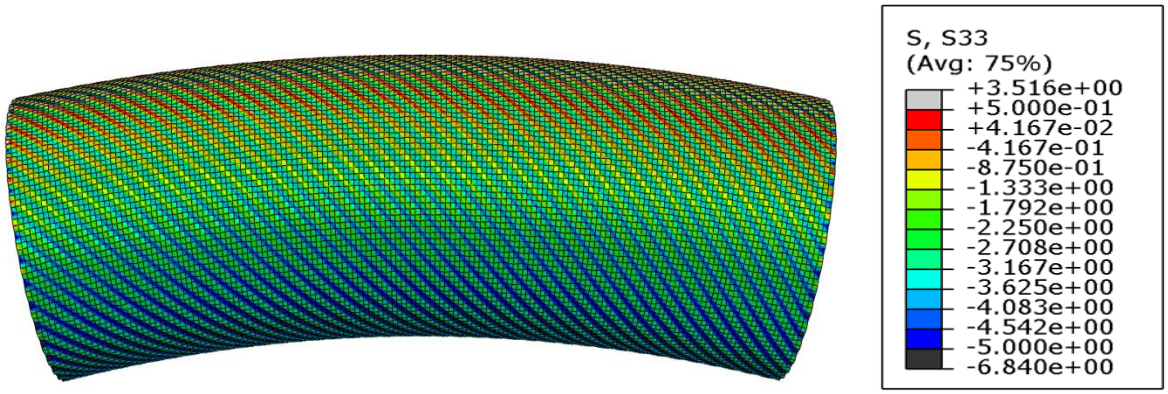

(b)

Figure 11: Axial stress on the inner layer using (a) fixed in-plane boundary conditions and (b) periodic boundary conditions.

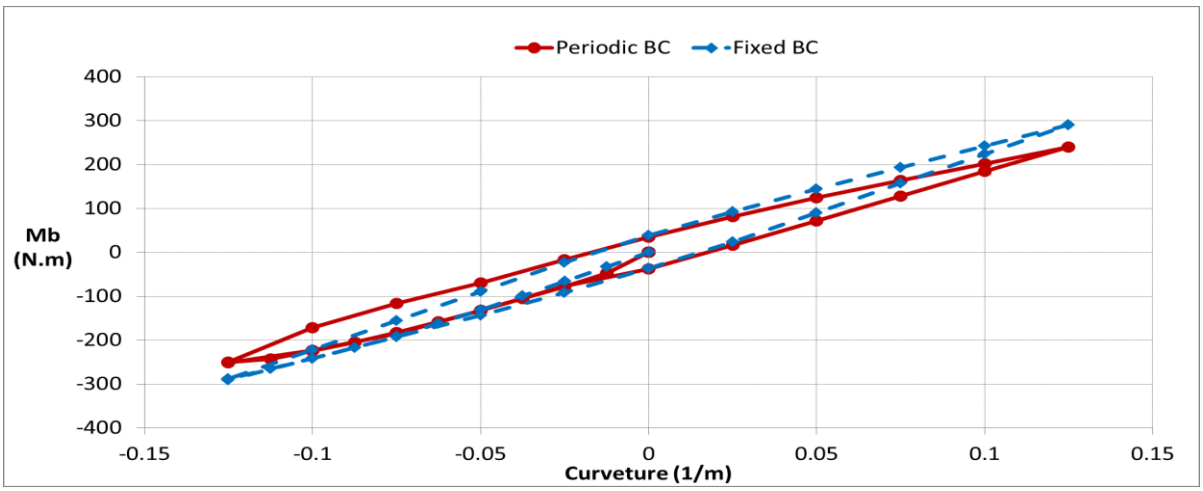

Figure 12: Bending moment hysteresis, 5 layers (internal pressure 4MPa, external pressure 4.5MPa).

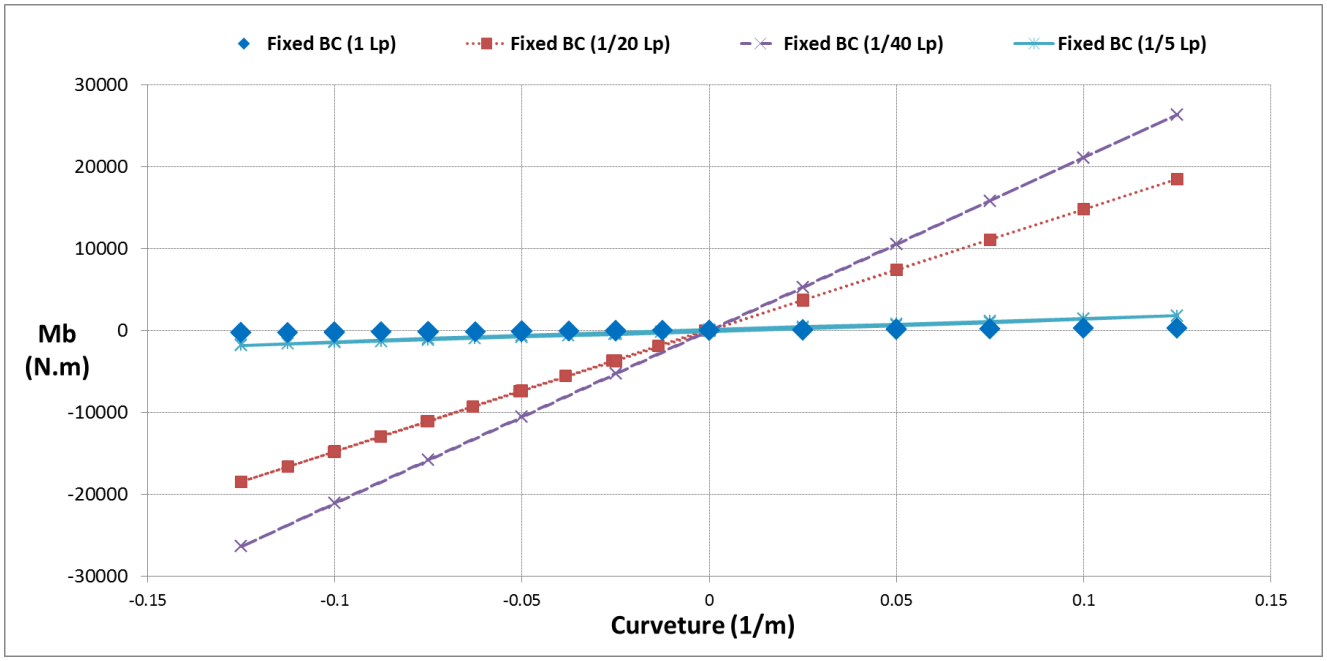

Figure 13: Comparison of bending moment hysteresis for models with various length (internal pressure 4MPa, external pressure 4.5MPa).

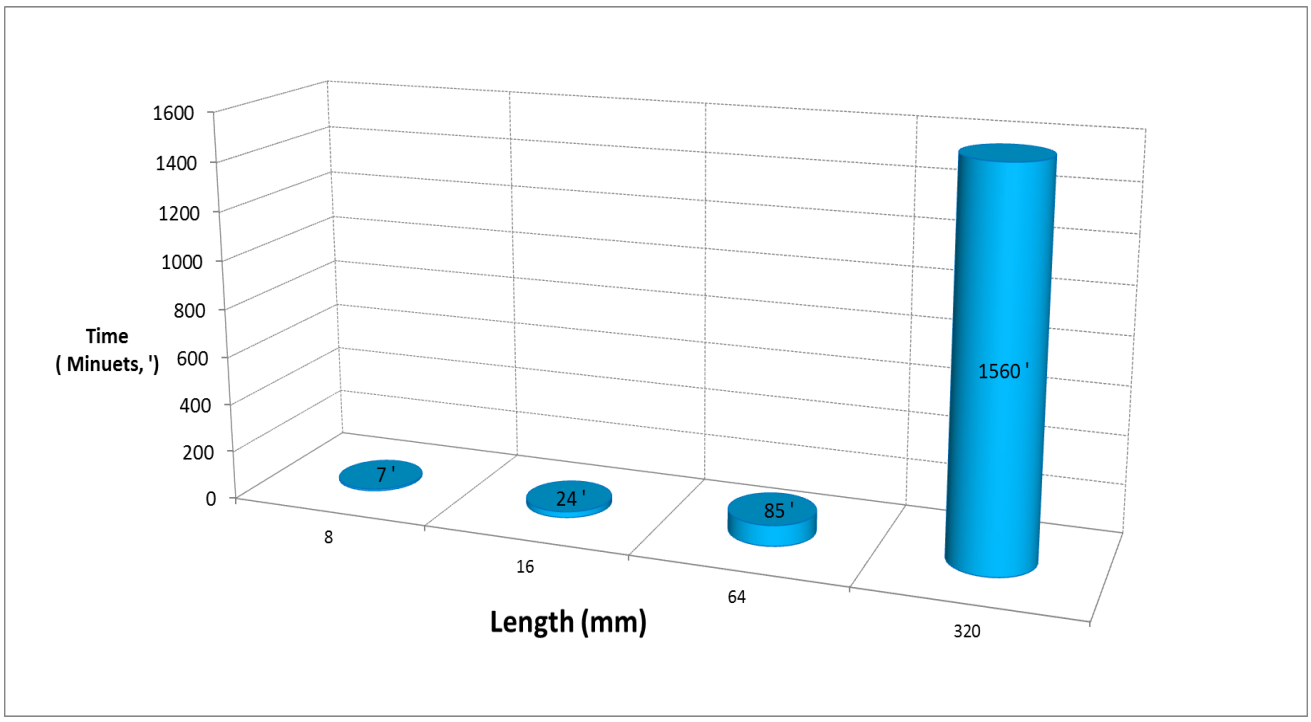

Figure 14: Computational cost for models with various lengths.

6. CONCLUSIONS

This paper has presented an approach to minimize the computational cost of a detailed nonlinear FE analysis of a segment of flexible riser, which includes all layers and accounting for frictional contact between them, so that it can be effectively used as the small-scale model a nested multi-scale analysis.

The key ideas behind the proposed approach are (a) the observation that flexible risers can be represented, with very good approximation, with a model having cyclic symmetry, (b) the use of such cyclic symmetry to reduce the length of the model to the smallest repeating unit and (c) the use of periodic boundary conditions.

Because of the possible non-uniqueness of the solution due to frictional contact, four models with lengths equal to 1, 2, 5 and 40 times the length of the repeating unit were considered, subjected to two set of values for the internal and external pressure and to prescribed cyclic variation of bending curvature. The difference in results across the four models is very small and can be attributed to small bifurcations in the numerical solution, not found in real life because of imperfections. On the other hand, the enormous saving in computational cost entailed by the use of the smallest repeating unit makes this the optimal model to be used in a nested (FE^2) multiscale analysis.

Further analyses reported confirm the importance of using periodic boundary conditions, particularly for the shorter length.

It is worth noting that precise cyclic symmetry implies lay angles which are almost but not precisely equal and opposite in the two armour layers, because, for the two armour layers, the pitch lengths are the same but their radii are different. More generally, this issue is related to the necessity to balance the torsional response of the two armour layers to avoid, or at least minimise, coupling between torsion and axial tension. The axial-torsional balance is normally obtained with a suitable combined choice of the lay angles, that often (but not always) are assumed to be equal and opposite, as well as the average radii of the armour layers, the cross sectional area of the tendons and their number. The cyclic symmetry considered in our work requires the same pitch length and the same number of tendons. Assuming the radii are dictated by the thickness of the anti-wear polymer layer, torsional balance can be still achieved by proper sizing of the tendon cross sections. For these cases, exact cyclic symmetry can be achieved in the design and the methodology presented in this paper can be applied.

On the other hand, some designs used in the industry do not perfectly satisfy cyclic symmetry to achieve axial-torsional decoupling. Therefore, future work will include the study of how to best approximate the small-scale problem with the assumption of cyclic symmetry in cases where cyclic symmetry is not exact in the real geometry.

Furthermore, while some successful experimental validation of a modelling approach that is similar to the one used in this paper has been presented by Leroy et al. [13], further experimental validation of our proposed numerical model will be an important part of the future developments of this research.

ACKNOWLEDGMENTS

The authors would like to acknowledge the financial support by EPSRC (grant EP/K034243/1).

REFERENCES

[1] Bahtui, H. Bahai, G. Alfano, 2009, “Numerical and analytical modelling of unbonded flexible risers”, Journal of Offshore Mechanics and Arctic Engineering, 131, 021401-1.

[2] Doan V.P. and Nishi Y., 2015 “Modeling of fluid–structure interaction for simulating vortex-induced vibration of flexible riser: finite difference method combined with wake oscillator model”, Journal of Marine Science and Technology, Volume 20, Issue 2, pp 309-321.

[3] de Sousa, J.R.M., Viero, P., Magluta, C., Roitman, N., 2010, “An experimental and numerical study on the axial compression response of flexible pipes”, Proceedings of the ASME 2010 29th International Conference on Ocean, Offshore and Arctic Engineering, OMAE2010-20856.

[4] Merino, H.E.M., de Sousa, J.R.M., Magluta, C., Roitman, N., 2010, "Numerical and experimental study of a flexible pipe under torsion", Proceedings of the ASME 2010 29th International Conference on Ocean, Offshore and Arctic Engineering, OMAE2010-20902.

[5] Le Corre, V., Probyn, I., 2009, "Validation of a 3-dimensional finite element analysis model of a deep-water steel tube umbilical in combined tension and cyclic bending", Proceedings of the ASME 2009 28th International Conference on Ocean, Offshore and Arctic Engineering, OMAE2009-79168 .

[6] Tan, Z., Quiggin, P., Sheldrake, T., 2007, "Time domain simulation of the 3D bending hysteresis behaviour of an unbonded flexible riser", Proceedings of the ASME 2007 26th International Conference on Ocean, Offshore and Arctic Engineering, OMAE2007-29315.

[7] Sævik, S., 2010, "Comparison between theoretical and experimental flexible pipe bending stresses", Proceedings of the ASME 2010 29th International Conference on Ocean, Offshore and Arctic Engineering, OMAE2010-20352.

[8] Sævik, S., 2011, "Theoretical and experimental studies of stresses in flexible pipes", *Computers and Structures*, 89, pp. 2273-2291.

[9] Alfano, G., Bahtui, A., Bahai, H., 2009, "Numerical derivation of constitutive models for unbonded flexible risers", International Journal of Mechanical Sciences, 51, 295-304.

[10] Peric, D., de Souza Neto, E.A., Feij_oo, R.A., Partovi, M., Molina, A.J.C., 2011, "On micro-to-macro transitions for multi-scale analysis of non-linear heterogeneous materials: unified variational basis and finite element implementation", International Journal for Numerical Methods in Engineering 87, pp. 149 -170.

[11] Hazanov, S., Amieur, M., 1995, "On overall properties of elastic heterogeneous bodies smaller than the representative volume", Int. J. Engrg. Sci. 33, pp. 1289-1301.

[12] Amieur, M., Hazanov, S., Huet, C., 1995, "Numerical and experimental assessment of the size and boundary conditions effects for the overall properties of granular composite bodies smaller than the representative volume", Parker, D., England, A. (Eds.), IAUTAM Symposium on Anisotropy, Inhomogeneity and Nonlinearity in Solid Mechanics, Kluwer Academic Publishers, Dordrecht. pp. 149-154.

[13] Leroy, J.M., Perdrizet, T., Le Corre, V., Estrier, P., 2010, "Stress assessment in armour layers of flexible risers", Proceedings of the ASME 2010 29th International Conference on Ocean, Offshore and Arctic Engineering, OMAE2010-20932.

[14] Edmans, B., Alfano, G., Bahai, H., 2012, "Large-scale analysis and local stress assessment of flexible unbonded pipes using FEA", Proceedings of the ASME 31st International Conference on Ocean, Offshore and Arctic Engineering, OMAE2012- 84249.

[15] Edmans, B., Alfano, G., Bahai, H., Andronicou, L., Bahtui, A., 2012, "Local stress assessment of flexible unbonded pipes using FEA", Proceedings of the ASME 31st International Conference on Ocean, Offshore and Arctic Engineering, OMAE2012-84248.

[16] Geers, M.G.D., Kouznetsova, V., Brekelmans, W.A.M., 2010, "Multi-scale computational homogenization: trends and challenges", Journal of Computational and Applied Mathematics 234(7), pp. 2175-2182.

[17] Edmans, B., 2012, "Non-linear Finite Element Analysis of Flexible Pipes for Deep-water Applications", Ph.D. thesis, Brunel University, London, UK.

[18] Edmans, G. Alfano, H. Bahai., 2013, "Nonlinear multi-scale homogenization with different structural models at different scales," International Journal for Numerical Methods in Engineering, 94(4): pp. 355-373.

[19] Rahmati, M.T., H. Bahai, G. Alfano, "Small-scale FE modelling for the analysis of flexible risers," OMAE2015-41825, ASME-OMAE 2015, St. John's, Canada, May 31-June 5, 2015.

[20] Hild, P., Renard, Y., 2005, "Local uniqueness and continuation of solutions for the discrete Coulomb friction problem in elastostatics", Quarterly of Applied Mathematics 63(3), pp. 553-573.

[21] Simulia. "ABAQUS User Manual", version 6.13.1.

[22] Haslinger, J., Janovský, V., Ligurský, T., 2012, "Qualitative analysis of solutions to discrete static contact problems with Coulomb friction", Computer Methods in Applied Mechanics and Engineering 205, pp. 205-208.